



## Study on the design of inlet and exhaust system of a stationary internal combustion engine

Ugur Kesgin \*

*Department of Naval Architecture, Mechanical Engineering Faculty, Yildiz Technical University,  
TR 34 349 Besiktas, Istanbul, Turkey*

Received 8 March 2004; received in revised form 22 June 2004; accepted 24 October 2004  
Available online 13 December 2004

---

### Abstract

The design and operational variables of inlet and exhaust systems are decisive to determine overall engine performance. The best engine overall performance can be obtained by proper design of the engine inlet and exhaust systems and by matching the correct turbocharger to the engine. This paper presents the results of investigations to design the inlet and exhaust systems of a stationary natural gas engine family. To do this, a computational model is verified in which zero dimensional phenomena within the cylinder and one dimensional phenomena in the engine inlet and exhaust systems are used. Using this engine model, the effects of the parameters of the inlet and exhaust systems on the engine performance are obtained. In particular, the following parameters are chosen: valve timing, valve diameter, valve lift profiles, diameter of the exhaust manifold, inlet and exhaust pipe lengths, and geometry of pipe junctions. Proper sizing of the inlet and exhaust pipe systems is achieved very precisely by these investigations. Also, valve timing is tuned by using the results obtained in this study. In general, a very high improvement potential for the engines studied here is presented.

© 2004 Elsevier Ltd. All rights reserved.

**Keywords:** Valve timing; Inlet pipe; Exhaust pipe; Junction; Natural gas engine; Efficiency

---

---

\* Tel.: +90 212 261 19 99/258 2157; fax: +90 212 261 66 59/258 2157.

E-mail addresses: [kesgin@yahoo.com](mailto:kesgin@yahoo.com), [kesgin@yildiz.edu.tr](mailto:kesgin@yildiz.edu.tr)

## 1. Introduction

For proper sizing of an exhaust pipe system of internal combustion engines, the following parameters are to be optimized: diameter and length of the pipes; material, thickness and insulation of exhaust pipe system; geometry of pipe connections (junctions); and position of the necessary elements of the exhaust system such as turbocharger, catalytic converter, silencer etc. The engine intake and exhaust systems determine the engine operational behavior in steady and transient modes, the engine performance and the engine emissions regarding exhaust gas and sound.

The design of exhaust and intake systems has been studied by numerous researchers [1–3]. For a higher engine efficiency and for a better engine performance in transient operation, the energy losses in the intake and exhaust systems, including the valves, of an engine are to be kept at a minimum. As an important design parameter, valve timing has been studied intensively [4–10]. Valve timing is to be designed to optimize engine performance at the engine operating range. Especially, variable valve timing decreases the problems of valve overlap and is used to reduce fuel consumption as well as exhaust gas emissions.

This can be accomplished by optimizing the heat transfer rates and pressure losses, particularly in the exhaust system, since higher temperatures and very complex gas flow phenomena occur in the exhaust system. The energy losses and flow instabilities in a pipe system occur particularly in pipe junctions. The energy losses in pipe junctions can be represented in engine cycle simulation by using pressure loss coefficients depending on the geometry of the junction, flow direction and mass flow rates. Accurate values of the pressure loss coefficients can be obtained experimentally as well as by analytical methods, for example one dimensional flow theory [11,12]. Kuo and Kalighi [13] performed a study to obtain flow loss coefficients for T shaped pipe junctions used in internal combustion (IC) engine exhaust systems numerically and experimentally. They showed that the flow loss coefficients are only mildly dependent on the cross-sectional shape. Klell et al. [14] give an alternative method to compute flow in pipe junctions. Their method is based on well known conservation laws such as mass, momentum and energy.

Turbocharging plays a crucial role to utilize exhaust gas energy efficiently. In order to increase the efficient use of exhaust gas energy, first, the gas is to be transported with minimum energy losses from the cylinders to the turbine. Then, this gas energy is to be converted at the turbine into mechanical work in the best possible way, which is needed by the compressor. Meier et al. [15] describe the “transmission or manifold efficiency” as the ratio of the exhaust gas energy given to the exhaust turbine to the exhaust gas energy at the cylinder exit.

Optimization of the exhaust pipe system aims to obtain higher transmission efficiencies in the engine operation range. Apart from obtaining higher transmission efficiency, by proper design of the engine exhaust system and by matching the correct turbocharger to the engine, the best engine overall performance can be obtained.

This paper deals with investigations to design the inlet and exhaust systems of a stationary natural gas engine family. In the framework of a detailed research and development project in co-operation with the university and industry, a gas engine series with 12, 16 and 20 cylinders, which is used in combined power plants, has been optimized regarding power, efficiency and emissions. Zero dimensional process calculations as well as one and multi-dimensional flow calculations are used for optimizing the gas exchange of these gas engines. Based on a precise comparison between measurements and calculations, extensive examinations for optimizing the gas exchange of V12,

V16 and V20 engines are performed. The results obtained here show a distinct optimization potential regarding valve timing, valve lift profiles, valve diameters, inlet and exhaust pipe lengths and exhaust manifold diameter as well as the geometry of the pipe junctions. The pipe junctions are optimized also by using a computational fluid dynamics (CFD) program system.

Finally, the results from the one dimensional and three dimensional computations are compared. The results from the three dimensional computations are also used for obtaining the flow coefficients of the optimized pipe junctions, and then, the effect of these optimized pipe junctions on the engine performance is obtained.

## **2. Computational tools for simulation**

Optimization of internal combustion engines is a trade off between engine efficiency, exhaust gas and noise emissions and engine operational behavior. Over the past decades, computational techniques have been used intensively to simulate the phenomena in internal combustion engines. These techniques permit very accurate results for engine performance and assessment of the effects of various operational and design parameters and manufacturing tolerances. These techniques offer also a cost effective alternative to the traditional practice of experimental prototype testing.

The computational methods used for engine development are the process calculations in the engine cylinder and the filling and emptying method as zero dimensional procedures and finite difference methods as one dimensional and multi-dimensional CFD methods. The methods used for optimization of the engines studied here are: as the zero dimensional method, the Motor Simulation and Evaluation System MOSES, which was developed at the institute for internal combustion engines and thermodynamics of the Technical University of Graz [16]; as the one dimensional procedure, the engine cycle simulation code BOOST [17]; and as the multi-dimensional procedure, the CFD code FIRE [18].

## **3. One dimensional gas flow simulation: finite differences**

The pulsating nature of the gas flow into and out of each cylinder creates significant gas dynamic effects, which require a more complete modeling approach than a zero dimensional model such as the filling and emptying method.

Gas dynamics models have been in use for many years to examine the whole processes in internal combustion engines. These models use the mass, momentum and energy conservation equations for unsteady compressible flow in the exhaust and inlet pipe systems. In the past, the method of characteristics was used to solve the gas dynamics equations. Finite difference methods for solving the one dimensional unsteady flow equations in intake and exhaust manifolds are proving more efficient and flexible than the method of characteristics [19].

The flow in a pipe of an engine exhaust and/or inlet system is treated as one dimensional. This means that the pressures, temperatures and flow velocities obtained from the solution of the gas dynamic equations represent mean values over the cross-section of the pipes. Flow losses due to three dimensional effects at particular locations in the engine are considered by appropriate flow

coefficients. The conservation equations for mass, momentum and energy can be written as follows [19]:

$$\frac{\partial}{\partial t} \begin{pmatrix} \rho \\ \rho U \\ \rho u \end{pmatrix} + \frac{\partial}{\partial x} \begin{pmatrix} \rho U \\ \rho U^2 + p \\ pU + \rho Uu \end{pmatrix} = \begin{pmatrix} -\rho U \frac{dA}{dx} \\ -\rho \frac{U^2}{A} \frac{dA}{dx} - \rho \frac{2\xi U|U|}{D} \\ -\frac{4h_c(T-T_w)}{D\rho} - \frac{1}{A} \frac{dA}{dx} \left( \frac{1}{2} \rho U^3 + \frac{\gamma}{\gamma-1} Up \right) \end{pmatrix} \quad (1)$$

where  $\rho$  is the gas density,  $t$  is time,  $U$  is the gas velocity,  $u$  is the specific internal energy of the gas,  $p$  is the pressure,  $A$  is the flow area,  $x$  is the coordinate,  $\xi$  is the friction coefficient,  $D$  is the equivalent diameter of the flow area,  $h_c$  is the convective heat transfer coefficient,  $T$  is the gas temperature,  $T_w$  is the wall temperature and  $\gamma$  is the ratio of specific heats.

The equations above have the vector form

$$\frac{\partial F}{\partial t} + \frac{\partial G}{\partial x} = H \quad (2)$$

where  $G$  and  $H$  are functions of  $F$  only. There are several finite difference methods used to solve these equations. The one step Lax–Wendroff method is used effectively for solving these equations. For this method, Eq. (2) can be developed into a Taylor series with respect to time with the space derivatives approximated by central differences around the mesh point  $j$  (see Fig. 1):

$$F_j^{n+1} = F_j^n - \frac{1}{2} \frac{\Delta t}{\Delta x} (G_{j+1}^n - G_{j-1}^n) + \Delta t H_j^n + \frac{1}{4} \left( \frac{\Delta t}{\Delta x} \right)^2 \left[ (G_{j+1}^n - G_j^n)(G_{j+1}^n - G_j^n) - (G_j^n - G_{j-1}^n)(G_j^n - G_{j-1}^n) \right] \quad (3)$$

where  $G' = \partial G / \partial F$ . This equation is first order accurate unless  $H$  is small. For stability in the integration process, the time step and mesh size must satisfy the CFL (Courant–Friedrichs–Levy) criteria as follows:

$$C = (|U| + a) \frac{\Delta t}{\Delta x} < 1 \quad (4)$$

where  $C$  is the Courant number and  $a$  is the sound speed for an ideal gas.

#### 4. Calculating inlet and exhaust system elements

Engine cycle simulation codes are widely accepted tools for performance prediction of engines at the design stage and for the analysis of existing engines. The engine cycle simulation code BOOST [17] provides well optimized simulation algorithms for all available elements in inlet and exhaust systems of an internal combustion engine including the cylinders.

The elements of an engine system are the cylinder, restrictions, fuel injector, pipe junctions, plenum with constant volume or with variable volume, air cooler, turbocharger, pipe end as system

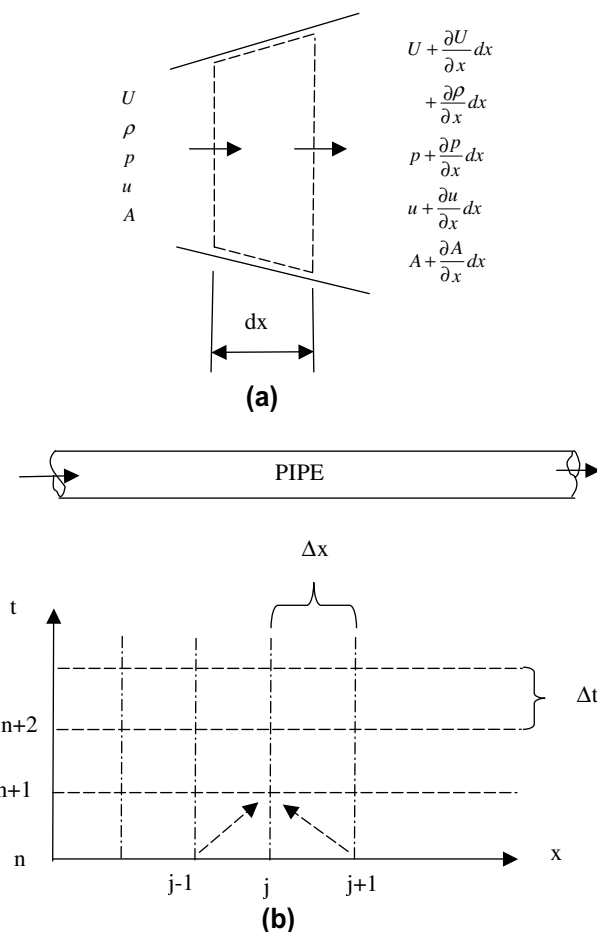


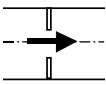
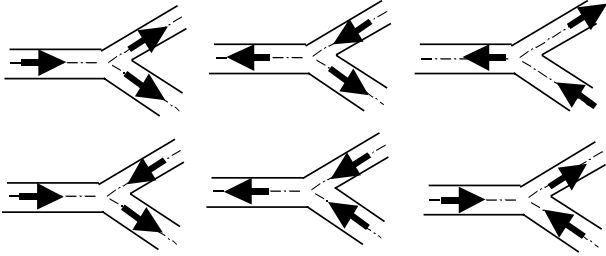
Fig. 1. (a) Control volume for unsteady one dimensional flow in a pipe. (b) Mesh for one step Lax–Wendroff method for one dimensional unsteady gas flow.

boundary, check valve, silencer, catalyst etc. These elements can be modeled with the corresponding models available in BOOST. Only a few of them will be described in the following to keep the paper length to a reasonable limit. Table 1 summarizes the necessary equations to calculate restrictions and pipe junctions [17,20,21].

#### 4.1. Calculating restrictions

As can be seen from Table 1, the calculation of the flow through a restriction is based on the conservation laws of energy and mass [17]. The mass flow rate through a restriction can be calculated by applying the energy equation for isentropic steady flow and assuming that the inlet velocity is negligible. The discharge coefficient of the restriction is adopted to consider the secondary flow effects, boundary layer separation, friction etc. [17,22].

Table 1  
Calculation restriction and pipe junction

Element	Equations	Definitions
Restriction	 $\dot{m} = \alpha_D \cdot A_{geo} \cdot p_{o1} \cdot \sqrt{\frac{2}{R_o \cdot T_{o1}}} \cdot \psi$ $\psi = \sqrt{\frac{\kappa}{\kappa - 1} \cdot \left[ \left( \frac{p_2}{p_{o1}} \right)^{\frac{2}{\kappa}} - \left( \frac{p_2}{p_{o1}} \right)^{\frac{\kappa+1}{\kappa}} \right]}$ $\frac{p_k}{p_{o1}} = \left( \frac{2}{\kappa + 1} \right)^{\frac{\kappa}{\kappa - 1}}$	$\dot{m}$ , mass flow rate $\alpha_D$ , discharge coefficient of restriction $A_{geo}$ , geometrical flow area $p_{o1}$ , upstream stagnation pressure $T_{o1}$ , upstream stagnation temperature $R_o$ , gas constant $\psi$ , pressure function $p_k$ , critical pressure $\kappa$ , ratio of specific heats
Possible flows in a pipe junction		
Mass balance:	$\frac{dm_J}{dt} = 0 = \sum_{input} \dot{m}_i - \sum_{output} \dot{m}_o$	$m_J$ , $E_J$ , mass and energy in the junction, respectively $\dot{m}_i$ , mass flowing into the junction $\dot{m}_o$ , mass flowing out of the junction
Energy balance:	$\frac{dE_J}{dt} = 0 = \sum_{input} \dot{m}_i \cdot h_{Ti} - \sum_{output} \dot{m}_o \cdot h_{To}$	$h_{Ti}$ , total enthalpy of the in-flowing mass $h_{To}$ , total enthalpy of the mass leaving the junction

#### 4.2. Calculating pipe junctions

A refined junction model for three pipe junctions is available in BOOST. In this case, it distinguishes between six possible flow patterns in the junction, as shown in Table 1. For each of the flow paths indicated in this figure, the equation for restriction flow is solved using values for the flow coefficients from a database provided with BOOST. These flow coefficients were obtained from steady state flow tests of junctions with different pipe diameters and different branching angles. The mass flow rates in the junction as well as the Mach number were also varied during these tests [17]. Table 1 shows the conservation equation of mass and energy in a pipe junction.

## 5. Calculating cylinder processes: one zone combustion model

Using a one zone combustion model, the first law of thermodynamics and the mass balance for the cylinder content are written in Table 2. Gas properties such as specific volume, internal energy and enthalpy of air, unburned fuel vapor and combustion gas are calculated for any time step at the cylinders, at every element and in every cell of the pipes. In addition to the mass concentration of the combustion gas, also its composition (air/fuel ratio) is determined. From this actual gas composition, the gas properties are computed. The composition of the combustion gases is obtained from chemical equilibrium considerations, including dissociation at the high temperatures in the cylinder. From this approach, the gas properties of the combustion gas are obtained depending on the pressure, on the temperature and on the air excess ratio [17].

For calculating the mass flow rates through the valves, the heat transfer in the valve channels is also considered. This heat transfer can be calculated by using the Zaph equation [23].

Heat is transferred through the surfaces of the piston, cylinder head and cylinder liner. The heat transfer through the walls can be represented as follows:

$$\frac{dQ_w}{d\alpha} = \sum_{i=1}^3 A_i \alpha_{HT} (T - T_{w_i}), \quad i = 1 \text{ piston}, i = 2 \text{ cylinder head}, i = 3 \text{ cylinder liner} \quad (5)$$

where  $A_i$  and  $T_{w_i}$  are the surface area and the surface temperature of the corresponding element, respectively,  $\alpha_{HT}$  is the heat transfer coefficient and  $T$  is the temperature of the cylinder content. This coefficient, which depends on the pressure and temperature and engine parameters, can be calculated by using the Woschni, Annand, Hohenberg etc. equation [23].

The model described here assumes that the gas mixture in the cylinder is perfect. By using this assumption, the ideal gas law for the cylinder content can be written as follows:

$$p_C V = m_C R T \quad (6)$$

where  $R$  is the gas constant.

The mass burned fraction,  $x$ , which represents the combustion, can be modeled either by given heat release percentages point by point over crank angle or by using a Vibe function, which is defined by the start of combustion, the combustion duration and a shape parameter, also called the form factor,  $m$  [23].

$$x = 1 - e^{6.908 \left( \frac{x}{\alpha_0} \right)^{m+1}} \quad (7)$$

where  $\alpha_0$  is the duration of combustion.

By using Eqs. (5)–(7) and the equations listed in Table 2 and other thermodynamical relationships [24], a set of ordinary differential equations is obtained, which can be solved with respect to the following variables as a function of crank angle:  $p_C$ ,  $T_C$ ,  $m_C$ ,  $x$ ,  $V$ ,  $Q_F$ ,  $Q_W$ ,  $W$ . The details of obtaining this set of differential equations can be found elsewhere [17,22–24]. This set can be solved numerically by using a Runge–Kutta method.

Table 2

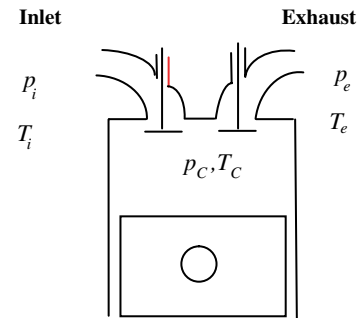
## Process calculation in cylinder

## First law of thermodynamics

$$\frac{d(m_C u)}{dz} = -p_C \frac{dV}{dz} + \frac{dQ_f}{dz} - \sum \frac{dQ_w}{dz} + \sum \frac{dm_i}{dz} h_i - \sum \frac{dm_e}{dz} h_e$$

## Mass balance

$$\frac{dm_C}{dz} = \frac{dm_i}{dz} + \frac{dm_f}{dz} - \frac{dm_e}{dz} - \frac{dm_{\text{Leak}}}{dz}$$



## Mass flow rate through valves

$$\frac{dm_{i,e}}{dt} = A_{\text{eff},i,e} \cdot \frac{p_{i,C}}{\sqrt{R \cdot T_{i,C}}} \cdot e^{-\bar{q}_{i,e}} \cdot \sqrt{\frac{2 \cdot \kappa}{\kappa - 1} \cdot \left[ \left( \frac{p_{C,e}}{p_{i,C}} \right)^{\frac{2}{\kappa}} - e^{\bar{q}_{i,e}} \cdot \left( \frac{p_{C,e}}{p_{i,C}} \right)^{\frac{\kappa+1}{\kappa}} \right] + q_{i,e} \cdot \left( \frac{p_{C,e}}{p_{i,C}} \right)^{\frac{2}{\kappa}} \cdot \frac{\rho_{i,e}}{p_{i,e}}}$$

Indices: C, cylinder; i, inlet valve; e, exhaust valve

$\frac{d(m_C u)}{dz}$ , change of the internal energy in the cylinder

$-p_C \frac{dV}{dz}$ , piston work

$\frac{dQ_f}{dz}$ , fuel heat input

$\sum \frac{dQ_w}{dz}$ , wall heat losses

$\sum \frac{dm_i}{dz} h_i$ , energy input into the cylinder through inlet valve

$\sum \frac{dm_e}{dz} h_e$ , energy output from the cylinder through exhaust valve

$\bar{q}_{i,e} = \frac{2 \cdot q}{c_p \cdot (T_{i,C} + T_{C,e})}$ , heat transfer factor through valve channel

$A_{\text{eff}} = C_D \cdot \frac{\pi \cdot d_v^2}{4}$ , effective flow area of the valve

$m_C$ , mass in cylinder

$u$ , specific internal energy of cylinder

$\alpha$ , crank angle

$p_{i,C,e}$ , inlet/cylinder/exhaust pressure

$T_{i,C,e}$ , inlet/cylinder/exhaust temperature

$V$ , cylinder volume

$Q_f$ , energy of fuel supplied into cylinder

$Q_w$ , wall heat loss

$m_i$ , mass inducted into cylinder

$h_i$ , enthalpy input into cylinder through inlet

$m_e$ , mass exhausted from cylinder

$h_e$ , enthalpy exhausted from cylinder

(continued on next page)



Table 2 (continued)

---

$m_f$ , mass of fuel burned
$m_{\text{Leak}}$ , mass of leakage
$C_D$ , valve flow coefficient
$d_{vi}$ , valve diameter
$q_{i,e}$ , heat transfer in inlet/exhaust channel
$C_p$ , specific heat at constant pressure
$R$ , gas constant
$\kappa$ , ratio of specific heats

---

## 6. Three dimensional flow simulation

### 6.1. Mathematical framework

A set of non-linear differential equations that describes the conservation of mass, momentum (3 velocity components) and energy forms the basis of a CFD analysis. In this analysis, it is possible to resolve every detail of an unsteady and turbulent flow and it is, therefore, common practice in CFD to compute time or ensemble averaged values of the variable in question. This is achieved by replacing the instantaneous values of the dependent variables (designated by the symbol  $\phi$ ) by the sum of an ensemble average value ( $\langle\phi\rangle$ ) and a variation ( $\phi'$ ) about this value [18]

$$(\phi = \langle\phi\rangle + \phi') \quad (8)$$

Replacement of the instantaneous quantities in the conservation equations for momentum, continuity and thermal energy by averages of the mean and fluctuating components leads to the following set of equations in Cartesian tensor notation [18].

Conservation of mass:

$$\frac{\partial \bar{\rho}}{\partial t} + \frac{\partial}{\partial x_j} (\bar{\rho} \cdot \bar{u}_j) = 0 \quad (j = 1, 2, 3) \quad (9)$$

Conservation of momentum:

$$\frac{\partial}{\partial t} (\bar{\rho} \cdot \bar{u}_i) + \frac{\partial}{\partial x_j} (\bar{\rho} \cdot \bar{u}_i \cdot \bar{u}_j + \bar{\rho} \cdot \overline{u'_i \cdot u'_j} - \bar{\tau}_{ij}) + \frac{\partial p}{\partial x_i} - \bar{\rho} \cdot g \cdot \frac{x_i}{|x|} = 0 \quad (10)$$

In this equation,  $u_j$  is the velocity component along the Cartesian coordinate direction  $x_j$ ,  $p$  is pressure,  $\rho$  is density,  $g$  is gravity acceleration and the stress tensor components  $\tau_{ij}$  have been grouped with certain fluctuating quantities in the following equation. Fluctuations in density and laminar viscosity have been ignored, as these are negligible in non-reacting turbulent flows.

$$\bar{\tau}_{ij} = \mu \cdot \left[ \frac{\partial \bar{u}_i}{\partial x_j} + \frac{\partial \bar{u}_j}{\partial x_i} - \frac{2}{3} \cdot \frac{\partial \bar{u}_m}{\partial x_m} \cdot \delta_{ij} \right] \quad (11)$$

Convention: Cronecker Delta  $\delta_{ij}$ :  $\delta_{ij} = 0$  for  $i \neq j$  and  $\delta_{ij} = 1$  for  $i = j$ .

Conservation of energy:

$$\frac{\partial}{\partial t}(\bar{\rho} \cdot h) + \frac{\partial}{\partial x_j} \left( \bar{\rho} \cdot \bar{u}_j \cdot \bar{h} + \bar{\rho} \cdot \overline{u'_j \cdot h'} \right) - \frac{\partial}{\partial x_j} \left[ \frac{\bar{\lambda}}{c_p} \cdot \frac{\partial \bar{h}}{\partial t} \right] - \frac{\partial \bar{p}}{\partial t} = 0 \quad (12)$$

$$\bar{h} = \bar{c}_p \cdot \bar{T} + \frac{1}{2} \cdot \bar{u}_i^2 \quad (13)$$

where  $h$  is total enthalpy,  $c_p$  is specific heat at constant pressure and  $T$  is temperature.

Furthermore, turbulent flows are characterized by a widely disparate set of length and time scales. A direct numerical solution of the equations would require a very fine discretization of space and time. For practical applications, the methodology involving direct solution of the conservation equations is currently not feasible, even with today's largest supercomputers.

These difficulties are resolved by expressing the flow variables in the governing equations by mean and fluctuating components. The subsequent averaging process generates unknown correlations, the average products of the fluctuation components. The formulation of expressions for the unknown correlations in terms of known or derivable quantities is called “turbulence modeling”. These expressions can be algebraic or differential equations, which depend upon the complexity of the turbulence model selected. In the case of the currently most popular  $k$ – $\varepsilon$  turbulence model, two differential equations have to be added to the equation system. In the case of a full Reynolds stress closure, the system is extended by seven differential equations [18].

## 6.2. Numerical solution procedure

All equations of the aforementioned system are derived for a general curvilinear non-orthogonal coordinate system. The individual terms of the partial differential equations are replaced by an algebraic approximation obtained by integrating over a control volume of finite size, this being identified with a cell of a computational grid superimposed upon the flow field. This procedure, known as the finite volume discretization scheme, leads to a set of non-linear algebraic equations linking the values of the dependent variables such as the velocities, pressure etc. to the centers of the computational grid. A typical CFD solution procedure consists of the following major steps [18]:

1. Increase time step.
2. Assemble coefficients of momentum equations and solve momentum equations.
3. Assemble coefficients and solve pressure correction equation to ensure that mass flow is conserved in a cell (continuity equation). The coupled momentum and pressure correction equations are solved with an algorithm based on SIMPLE (Semi-Implicit Method for Pressure Linked Equations).
4. Correct the velocity, pressure and density.
5. Assemble coefficients of the equations of the selected turbulence model and solve these equations.
6. Calculate coefficients for the enthalpy equation, solve enthalpy equation and update temperature and density.
7. Check for convergence, if not, repeat steps 2–7, otherwise start next time step, repeat steps 1–7.

Detailed information on three dimensional flow simulation and numerical solution procedures of this type of simulation can be found in the open literature [18,25].

## 7. Calculation of an engine—one dimensional engine model

The effect of the inlet and exhaust systems on the engine performance can be obtained numerically at least by using a one dimensional engine model. To develop this engine model, the engine cycle code BOOST is utilized. Then, this engine model is verified by comparisons with experiments including pressure-time history in the cylinders and at various locations of the engine exhaust turbocharging system. In such a computational model of a real engine, the numerical or geometrical simplifications and assumptions used in the computational model cause very large uncertainties. To examine these influences of the open model parameters on the engine performance, sensitivity analyses are executed. Thus, a good agreement with the experimental results is obtained [20]. After this verification, a parametric study for obtaining the effects of the turbocharging system is performed.

The engine model studied here is based on a V16 mixture loaded, lean burn gas engine with 1500rpm whose technical data are listed in Table 3. Because the engine has one turbocharger per cylinder row; only one cylinder row in the model is considered (Fig. 4). The model consists of eight cylinders, one turbocharger, one mixture cooler, four pipe ends (2 of them are closed, 2 of them are open), 56 pipes, 16 pipe junctions, 19 restrictions, a fuel injector and three pressure measuring points; one is in cylinder 1, one is at the end of the exhaust pipe and the last one is at the location before the exhaust gas turbine.

The presentations and comparisons hereafter are made by using the engine efficiency, volumetric efficiency, trapping efficiency, residual gas fraction, mean effective pressure and mean effective pressure for gas exchange, whose definitions are summarized in Table 4 [17,28].

## 8. Comparison of measurement and calculation

The measurements are executed at an efficient, modern test stand. There are also three measuring points on the real engine according to the engine model mentioned above. These are as follows: one is in cylinder 1, one is at the end of the exhaust pipe and the last one is at the location before the exhaust gas turbine. A pressure-time history depending on crank angle is obtained at each of these measuring points. Also, additional integral values of the measured

Table 3  
Properties of gas engine series

Bore/stroke [mm/mm]	190/220
Number of cylinders	V12, V16, V20
Air excess ratio	>1.7
Mean eff. pressure [bar]	16
Compression ratio [–]	11
Number of valves	2 exhaust, 2 inlet

Table 4  
Gas exchange characteristics

Characteristic	Equation
<i>Engine (thermal) efficiency</i> , $\eta$ , is defined as the work done per cycle, $W$ , divided by the fuel energy supplied to the engine per cycle	$\eta = \frac{W}{m_f q_{LHV}}$  $m_f$ , mass of fuel supplied into the engine per cycle $q_{LHV}$ , lower heating value of the fuel
<i>Volumetric efficiency</i> ( $\eta_{vol}$ ) as another performance parameter of importance is defined as the mass of fuel, and air inducted into the cylinder divided by the mass that would occupy the displacement volume at the density related to ambient conditions. Note that the volumetric efficiency is a mass ratio not a volume ratio	$\eta_{vol} = \frac{m_a + m_f}{\rho_o V_d}$  $m_f$ , mass of fuel $m_a$ , mass of air $V_d$ , displacement volume $\rho_o$ , density at ambient conditions
<i>Residual fraction</i> ( $x_r$ ) is the rate of residual mass left over from the previous cycle to the mass of air (or mixture) retained	$x_r = \frac{m_f}{m_a + m_f}$
<i>Trapping efficiency</i> ( $\Gamma$ ) is the rate of mass of delivered air (or mixture) retained to the mass of delivered air (or mixture)	$\Gamma = \frac{m_a + m_f}{m_{delivered}}$
<i>The mean effective pressure</i> (mep), which scales out the effect of the engine size, is the work done per unit displacement volume	$mep = \frac{W}{V_d}$
<i>The mean effective pressure for gas exchange</i> (GE-mep) is the work done during gas exchange processes, $W_{GE}$ , per unit displacement volume	$GE - mep = \frac{W_{GE}}{V_d}$

values like general engine characteristics, turbocharger's data, temperatures and pressures for oil and cooling systems, exhaust gas emissions etc. were determined and consulted by these measurements for comparison of the computational results with those from measurement.

For these three pressure measurements, piezoelectric pressure transducers are used. The transducer in cylinder 1 has a resolution of 0.004 bar, and the transducers in the exhaust pipe have a resolution of 0.0002 bar. These pressure transducers performed a pressure-time history. There are also numerous temperature measurements from the engine, some of them are already listed in Table 5. The accuracy of the temperature measurements is around 1 K.

The engine process in cylinder 1 is calculated by using a zero dimensional model, which is described in Section 5. The combustion is computed by given heat release percentages point by point over crank angle. To obtain the heat release percentages, the pressure-time history measured within cylinder 1 and other necessary data from experiments are analyzed by using MOSES.

Table 5 shows a comparison of the calculations with measurements. Note the agreement with respect to amplitude, frequency and harmonic content. This good agreement acknowledges both the high accuracy of the computational method used here and the reality of the selected variables in the engine model. According to the engine model in Fig. 2, the pressures for the three measurement points depending on crank angle prove the validity of the computational model clearly (Fig. 2). Because the engine model is verified by comparisons with experimental results, it can be

Table 5  
Comparison of measurements and calculation

Value	Computed $C$	Measured $M$	Relative error [%] $\frac{ C-M }{M} \times 100$
Pressure before compressor (bar)	0.906	0.903	0.33
Temperature before compressor (K)	289	290	0.35
Pressure after compressor (bar)	2.620	2.620	0.00
Temperature after compressor (K)	414	419	1.21
Pressure after gas throttling (bar)	2.558	2.555	0.12
Temperature after gas throttling (K)	324	324	0.00
Pressure before turbine (bar)	2.063	2.042	1.02
Temperature before turbine (K)	846	839	0.83
Pressure after turbine (bar)	0.983	0.999	1.63
Temperature after turbine (K)	736	706	4.08
Mean effective pressure <sup>a</sup> (bar)	15.59	14.05	9.88
Excess air ratio (–)	2.04	2.04	0.00
Indicated thermal efficiency—engine (%)	39.8	39.7	0.25
Amount of fuel (g/s)	44.70	44.76	0.13

<sup>a</sup> Mean effective pressure shows indicated value for calculation and effective value for measurements; also the difference represents the friction losses. The relative difference of 9.88% means that the engine has a mechanical efficiency of approx. 90%.

considered sufficiently reliable to investigate the effect of the engine geometrical and operational parameters and to design new engine concepts.

## 9. Effect of inlet and exhaust piping on engine performance

In the following, the effect of the geometry of the inlet and exhaust pipe systems on the engine performance of the V12, V16 and V20 engines are examined. In particular, the effects of the exhaust manifold diameter, the exhaust and inlet pipe lengths as well as the pipe junction geometry on engine performance are discussed. The latter is investigated by using one dimensional as well as three dimensional simulation. The results of these investigations are presented in the following.

### 9.1. Effect of the length of inlet pipes (runners)

The effect of the length of inlet pipes is obtained using BOOST. For this investigation, all engine parameters are left unchanged, and only the inlet pipe length is varied. These investigations show that the engine efficiency decreases slightly with increasing length of inlet pipes (Fig. 3). The reason for this decrease is the decrease in the gas exchange mep.

### 9.2. Effect of the exhaust manifold diameter

For this gas engine family, constant pressure turbocharging was selected as the loading system. In order to achieve a good approximation to the ideal constant pressure turbocharging, also the diameter of the exhaust manifold is to be optimized.

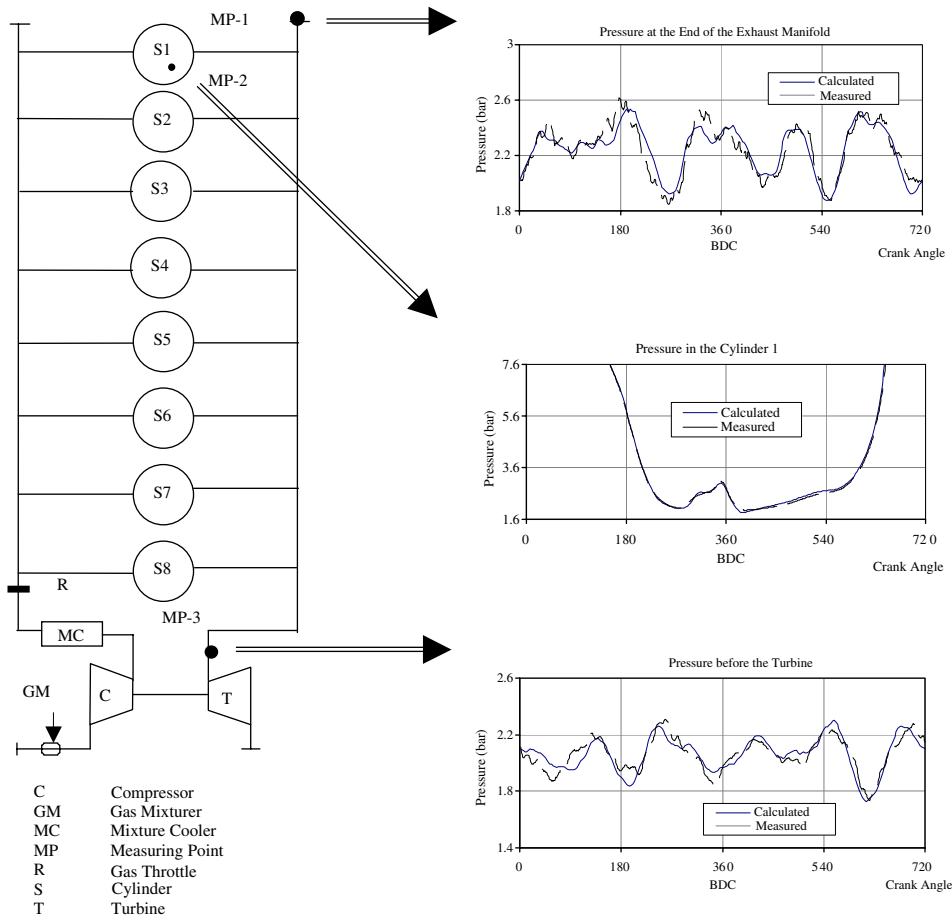


Fig. 2. Calculation model of the V16 engine and comparison of calculation and measurement for the pressures at the end of the exhaust manifold, in cylinder 1 and before the exhaust turbine.

In order to clarify the influences of the diameter of the exhaust manifold, variations were executed from approximately 70–116% of the cylinder bore. The results regarding indicated thermal efficiency (engine efficiency), indicated mean effective pressure, indicated mean effective pressure for gas exchange process and the pressure in the exhaust manifold and in the cylinder of the V20 engine are presented in Fig. 4. This figure shows that the indicated thermal efficiency and also the indicated mean effective pressure increase with rising pipe diameter. Considering that the base engine has an exhaust pipe diameter of approximately 132 mm, which is equal to around 0.7 times the cylinder bore, sizing the pipe with a diameter equal to the cylinder bore (here 190 mm) brings an increase of approximately 0.7% point in the engine efficiency. An exhaust pipe with a larger diameter than the cylinder bore, in other words a greater value than 1.0 for the ratio of exhaust pipe diameter to cylinder bore, brings a negligible increase in the engine efficiency but also results in an increase of engine size. Therefore, the ratio of 1.0 for the V20 engine can be considered as an optimal value.

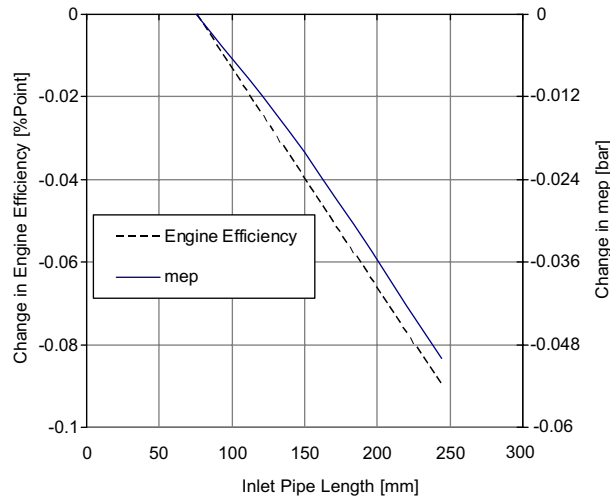


Fig. 3. Effect of the inlet pipe length on the engine efficiency and mean effective pressure (mep).

In fact, the optimal ratio of the exhaust manifold diameter to the cylinder bore depends on the number of cylinders, which are related to the exhaust gas amount, and on the engine load. If one regards the V12 engine at the same operating point, the indicated thermal efficiency achieves its maximum at the point of 0.9 (i.e. an exhaust manifold diameter of 170 mm), which is a smaller ratio than that for the V20 engine.

Fig. 4b shows the pressure-time history within the cylinder during the exhaust process for various exhaust manifold diameters. It can be seen from this figure that the pressure level decreases as the exhaust manifold diameter increases, and thus, the piston spends less effort to push the exhaust gases out of the cylinder. This brings an increase in the engine efficiency.

### 9.3. Effect of length of exhaust pipes

A further constructional parameter, whose influences are to be examined on the engine performance, is the exhaust pipe length between the cylinder head and the exhaust manifold. To obtain these influences, a parametric study is performed for the V20 engine. The results show that the engine efficiency increases with elongation of the exhaust pipes (Fig. 5).

The elongation of the exhaust pipes results in an increase of the wave running time between the cylinders, and thus, the interactions between cylinders decrease. This means a profit on the mean effective pressure as well the engine efficiency. For example, if one increases the exhaust pipe length from 62 mm to 1.5 m, an increase of the efficiency of 0.38% points is obtained. Exhaust pipes longer than 1.5 m lead to no further improvement of the efficiency.

Elongation of the exhaust pipes also has a few disadvantages such as increasing the engine size and, thus, constructional complexity, which is a trade off between engine efficiency and compact engine size. Also, the maintenance work of the engine is to be considered as another design criterion.

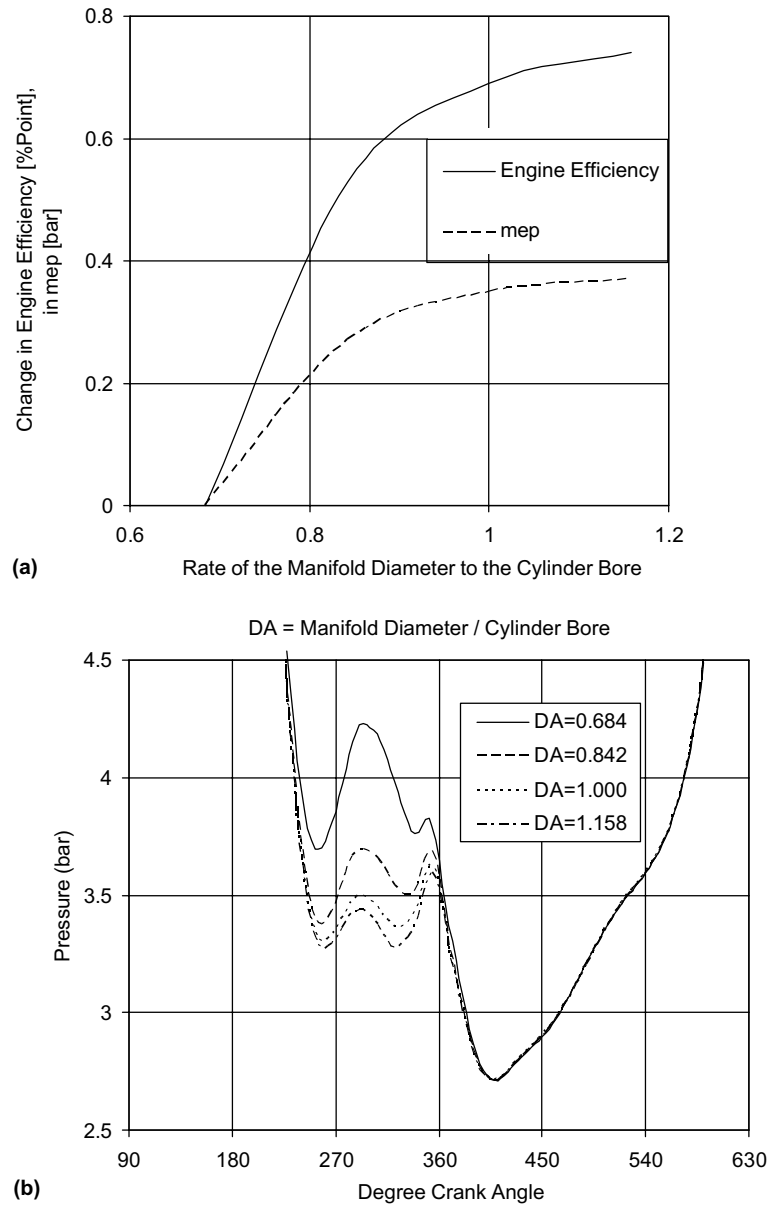


Fig. 4. (a) Effect of the exhaust manifold diameter on the engine efficiency and mean effective pressure (mep) and (b) cylinder pressures for different exhaust manifold diameters.

#### 9.4. Effect of pipe junction geometry: 1D simulation

A pipe junction is a unification of more than two pipes in a pipe system. The geometry of the pipe junction in an exhaust system influences the flow characteristics and the efficiency of the exhaust gas turbocharging.



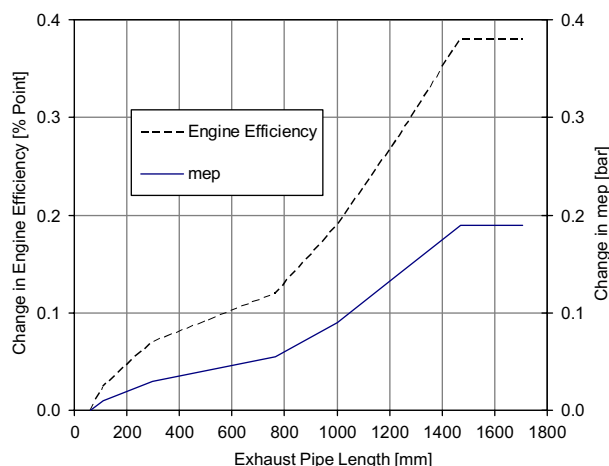


Fig. 5. Effect of the length of the exhaust pipe on the engine efficiency and mean effective pressure (mep).

The influence of the exhaust pipe length was already discussed in the previous section. The fact is remarkable that the efficiency rises on elongation of the exhaust pipes up to a length of approx. 1.5 m. An exhaust pipe length of 300 mm is chosen for further examinations. This length corresponds to a good compromise regarding the engine efficiency and the requirements for a compact engine size. This extension brings an increase of the engine efficiency around 0.08% points (see Fig. 6) and permits forming the exhaust pipes as a diffuser.

By considering the pressure of around 4 bar and the temperature of around 950 K in the exhaust pipes, one can estimate that the maximum value of the Reynolds number of the gas flow in the exhaust pipes is around  $\sim 10^6$ . At this Reynolds number of the exhaust gas flow, the maximum permissible extension angle of a diffuser is around  $\sim 6^\circ$ – $8^\circ$  [26].

Fig. 6 shows the effect of the diffuser extension angle of exhaust pipes with a length of 300 mm on the engine efficiency. The efficiency is increased around 0.07% point for the angle of  $8^\circ$ . Considering an elongation of exhaust pipes from 62 mm to 300 mm brings an increase of 0.08% points in the engine efficiency, while an elongated exhaust pipe with a diffuser extension angle of  $8^\circ$  results in a total increase of the engine efficiency of 0.15% points.

### 9.5. Effect of pipe junction geometry: 3D simulation

For the exact analysis of the exhaust gas piping system, it has proved appropriate to introduce its own efficiency definition for the enthalpy fed from the exhaust valve to the exhaust gas turbine. Meier et al. [15] describe the transmission efficiency or manifold efficiency as the ratio of the enthalpy of the exhaust gases entering the exhaust gas turbine to that of the gases leaving the cylinder. Accordingly, by the geometry of the pipe junctions, the transmission efficiency can be increased.

Another part of the optimization work is focused on the examination of the exhaust pipe junction influence on the engine behavior with the help of one and three dimensional calculation methods. In the following, the geometry of the pipe junctions optimized by 3D computing

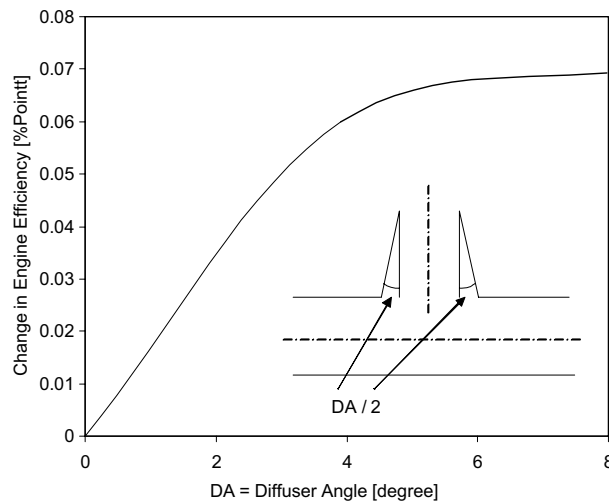


Fig. 6. Effect of the diffuser angle in the exhaust pipe junctions on the engine efficiency.

is presented. These investigations are conducted to obtain a large transformation of the kinetic energy into pressure energy by an appropriate shape, and thus, an improvement of the transmission efficiency of the exhaust gases can be obtained. On the other hand, the new geometry is not only to reduce the mutual disturbances of the cylinders but also to increase the engine efficiency.

#### 9.5.1. Geometry of pipe junctions

The branching angle under which the exhaust pipes are connected to the exhaust manifold is an important design parameter for pipe junctions. Since the flow conditions at the pipe junctions, in particular the effects of the branching angle, could not be fully described with a one dimensional method, the different junction geometries are examined with a CFD program, i.e. with FIRE-AVL List. Thus, a nearly exact simulation of the junctions is accomplished.

The previous examination with 1D simulation shows that the exhaust pipes are to be shaped in a diffuser form with a length of 300 mm. Considering the results from the 1D simulation, various geometries of exhaust pipe junctions are designed. In all the simulations, a diameter of the exhaust manifold of 190 mm is assumed. The diameter of the pipes connected to the cylinder head of 80.9 mm is left constant. Because of space limitations, just two of them will be discussed here. Their major characteristics are summarized as follows (see Fig. 7):

- In the exhaust gas geometry called basic variant, the exhaust pipes have a constant diameter from the cylinder head to the manifold and a branch angle to the manifold of  $90^\circ$  so that it is a T shape junction. The length of the exhaust pipes for geometry J1 is 300 mm.
- In geometry J2, the exhaust pipe is formed as a curved diffuser from the cylinder head to the exhaust manifold. The exhaust pipe has a branching angle of approx.  $50^\circ$  to the longitudinal axis of the exhaust manifold. The length of the stream path line in the longitudinal pipe axes from the cylinder head to the exhaust manifold is 300 mm.

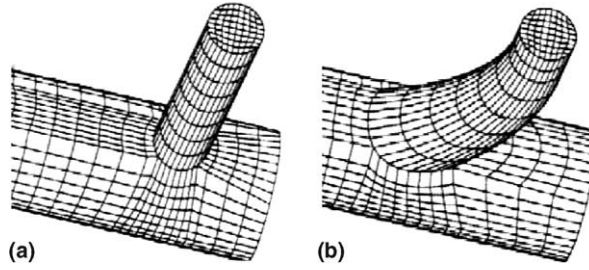


Fig. 7. 3D models of pipe junctions: (a) Junction J1 and (b) Junction J2.

### 9.5.2. Computer models and results of 3D simulation

Mass flows and temperatures from the cylinders, depending on time, are given as input boundary conditions. As output boundary condition, temporarily, the pressure at the turbine entrance is given. These boundary conditions are taken from the 1D simulation using cycle simulation code BOOST. The simulated time interval covers two complete engine cycles so that it is possible to illustrate the complex exhaust flow conditions at each time.

Fig. 8 shows the results of these 3D simulations regarding velocity field, pressure distributions and dissipation rate. This discussion will be given later. A time when the mass flow rate from the cylinder is the highest is selected for comparisons, because the flow conditions are crucial during this blow down phase for the losses at the pipe junction.

**GEOMETRY J1:** As it can be seen in Fig. 8a, a stagnation point forms at the entrance cross section facing the wall of the exhaust manifold. The maximum value of the static pressure occurring is around 0.6 bar more than the given pressure level. As a result of high velocity gradients, also a very high dissipation rate occurs within this region.

**GEOMETRY J2:** The geometry shaped into a diffuser form has advantages for a better transmission efficiency as well as for a higher engine efficiency. This version represents well optimized exhaust pipe geometry. The maximum value of the dissipation rate in this geometry lies in the entrance cross section and amounts only to around 10% of the value of that for geometry J1.

### 9.5.3. Evaluation of 3D simulation results

In this part of the study, it is aimed to obtain a higher manifold or transmission efficiency of the exhaust gas energy, which strongly depends on the energy losses in the whole exhaust piping system. Because a lesser energy loss means a higher transmission efficiency, the results of the CFD calculations were evaluated by considering the total enthalpy losses in the pipe junctions. In this case, the objective here is to optimize the exhaust pipe geometry to decrease the total enthalpy loss in the exhaust pipe system. The enthalpy losses are computed as follows.

The isentropic enthalpy change,  $\Delta \dot{H}_S$ , of the exhaust gases from the state of the exhaust condition to ambient pressure can be defined in such a way that

$$\Delta \dot{H}_S = \dot{m}_{EXH} \cdot [h_{EXH}(p_{EXH}, T_{EXH}) - h_{EXH,s}(p_A, s_{EXH})] \quad (14)$$

where  $\dot{m}_{EXH}$  is the exhaust gas flow rate,  $h_{EXH}$  is the enthalpy of the exhaust gas,  $h_{EXH,s}$  is the enthalpy of the exhaust gas after isentropic expansion to the ambient,  $p_{EXH}$  and  $T_{EXH}$  are the

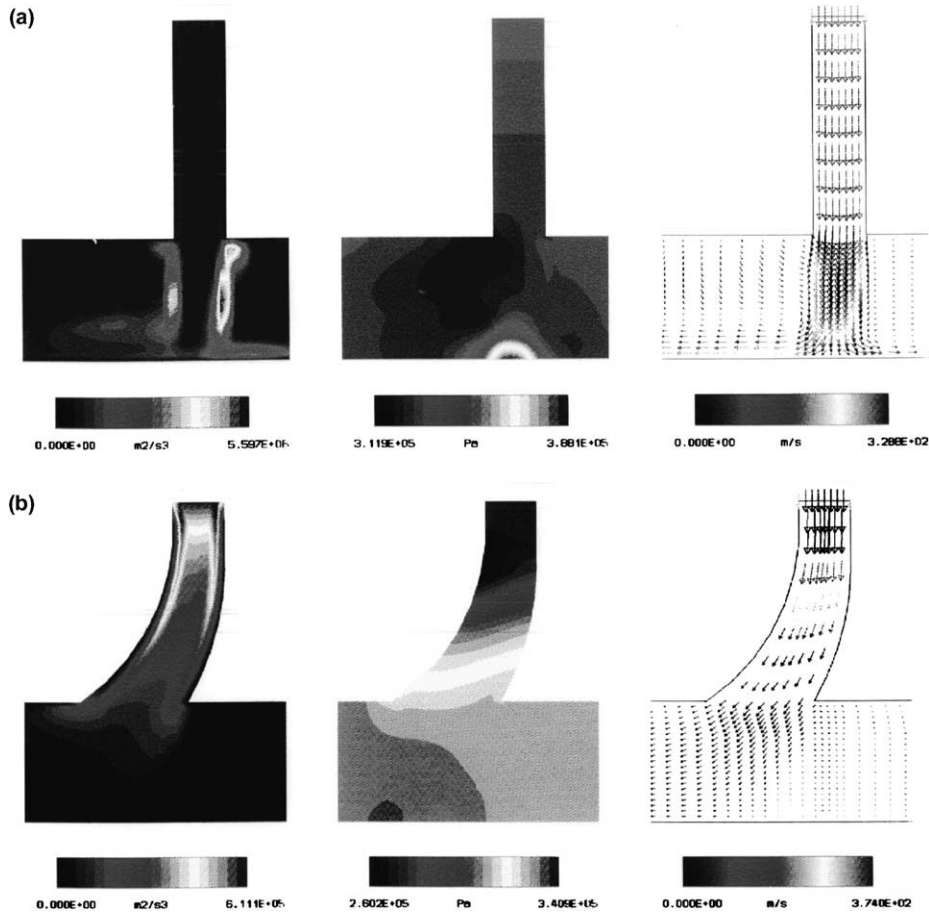


Fig. 8. Flow characteristics (left: dissipation, middle: pressure, right: speed) in pipe junctions: (a) Junction J1 and (b) Junction J2.

pressure and the temperature of the exhaust gas, respectively,  $p_A$  is the ambient pressure and  $s_{EXH}$  is the specific entropy of the exhaust gas.

Considering also the available kinetic energy,  $\dot{E}_K$ , the total isentropic enthalpy change,  $\Delta\dot{H}_{S,tot}$ , of the exhaust gases can be expressed as follows:

$$\dot{E}_K = \frac{1}{2} \dot{m}_{EXH} \cdot v_{EXH}^2 \quad (15)$$

$$\Delta\dot{H}_{S,tot} = \Delta\dot{H}_S + \dot{E}_K \quad (16)$$

where  $v_{EXH}$  is the velocity of the exhaust gas.

The enthalpy loss,  $\Delta\dot{H}_{LOSS}$ , is defined as the difference of the total isentropic enthalpy changes between the entrance and the outlet of the junction:

$$\Delta\dot{H}_{\text{LOSS}} = \sum_{\text{IN}} \Delta\dot{H}_{\text{S,tot}} - \sum_{\text{OUT}} \Delta\dot{H}_{\text{S,tot}} \quad (17)$$

It should be noted that the temporal enthalpies are integrated over the corresponding cross section flow area, and then, they are integrated over one engine cycle.

The results show that the enthalpy loss for the engine exhaust pipe system with geometry J2 is around 7.6% lower than that of the one with geometry J1. In other words, geometry J2 increases the transmission efficiency of the exhaust pipe system around 7.6%. To estimate the effect of this increase on the engine efficiency, the following approximation is used:

The geometry J2, as an optimized variant, results in an increase of the transmission efficiency of around 7.6%. This means that the energy of the exhaust gas given to the turbine is increased in the same percentage, i.e. 7.6%. Considering the efficiency of the turbocharger of this engine is 65%, an increase with a percentage of 7.6 represents an increase of around 5% in the turbocharger efficiency. Another study showed that an increase of the turbocharger efficiency of 1% point results in an increase in the engine efficiency of 0.07% points [21]. Considering this result, it can be said that an increase of the exhaust gas energy of 7.6% with geometry J2 brings an increase in the engine efficiency of 0.35% points. The effect of the geometry J2 on the engine efficiency is discussed further in the following section.

#### 9.5.4. Extension of the flow coefficient catalogue for 1D Simulation with BOOST

In order to estimate the effect of the junction J2 on the engine efficiency using the 1D program system BOOST, it is necessary to obtain the flow coefficients of the junction J2 because the flow coefficients catalogue of the program system BOOST does not include coefficients for this junction. The flow coefficients in this catalogue are indicated as a function of flow cross section area, branching angles of the pipes and mass flow rates in each pipe branch.

There are six different flow types in a pipe junction connecting three pipes. Three of them are dividing flows and three of them are combining flows, and also, the catalogue includes flow coefficients for each type of flow. Because of space limitations, a deeper discussion about the flow in pipe junctions will not be given here. Detailed information about flow and flow coefficients can be found in the literature [15,16,27].

The 3D geometrical model of junction J2 presented in Fig. 7 is modified to obtain steady state flow conditions within the junction so that the turbulence effects can be avoided for this type of junctions in which very complex flow phenomena occur. This modification is accomplished with elongation of the pipe branches from the junction. The necessary boundary conditions such as mass flow rate and temperature to compute these 3D stationary flow calculations are specified considering the mass flow rates at the exhaust flow conditions occurring in the real engine operation. The latter are known from the previous investigations explained already. The flow coefficients for each type of flow in junction J2 are calculated using these 3D results. For example, the coefficients for dividing flow are presented depending on the mass flow rate in Fig. 9.

The flow coefficients are used in the 1D program system BOOST to estimate the effect of junction J2 on the engine efficiency. The simulation with these flow coefficients in BOOST shows that junction J2 increases the engine efficiency around 0.3% points, which is slightly below the value of 0.35% points predicted by the method using total enthalpy change. This slight difference between these two predictions can be explained by the following: First, the 1D simulation can not describe

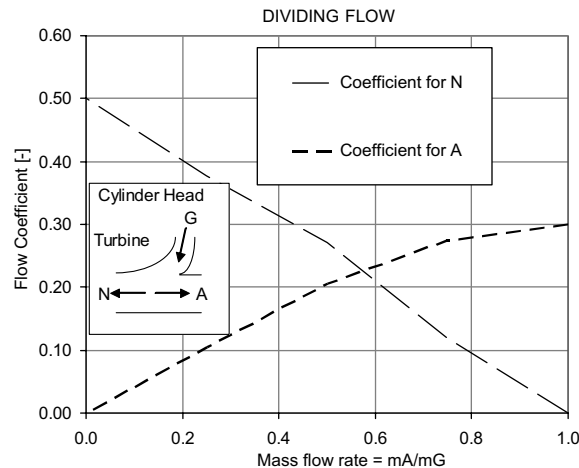


Fig. 9. Flow coefficients for dividing flow in the diffuser shaped T junction.

the very complex 3D flow conditions. Another reason is that the flow coefficients are determined under steady state conditions, but the flow occurring in a real engine is unsteady. This conflict could be solved by coupling one and three dimensional analysis of the engine. This coupling could be accomplished by using a 3D model for the entire exhaust pipe system and a 1D analysis for the rest of the engine. Chiavola [1] performed such an analysis using 1D and 3D simulation tools to simulate engine intake and exhaust systems.

## 10. Effect of valves on engine performance

The effect of valve timing, valve lift profiles and valve diameter on the performance of a V12 engine is investigated here. The engine model is the same as in Fig. 2 except the number of cylinders. The results of these investigations are discussed in the following.

### 10.1. Effect of valve timing

Valve timing has a great influence on the engine processes, especially the gas exchange process, and thus, the cylinder charge is directly affected. The valve overlap period at the top dead centre (TC), where the exhaust and intake valves are both open, creates a number of flow effects such as back flow of the exhaust into the inlet manifold when the exhaust pressure is greater than the inlet pressure. This back flow reduces the volumetric efficiency of the engine. On the other hand, since this dilution will reduce the peak combustion temperatures, the NO<sub>x</sub> emission will also be reduced [28]. When the intake pressure is greater than the exhaust pressure, this time, there will be some short circuiting of the inlet charge, which is a mixture of natural gas and air in the engines studied here, directly to the exhaust, and thus, a fraction of the fuel is not burning in the cylinder. This will first reduce the trapping efficiency of the engine and then the engine performance, since the unburned fuel energy is not converted into mechanical energy.

For turbocharged engines, the opening time of the exhaust valve plays an important role. If the exhaust valve opens too early, more than necessary work is lost in the later stages of the power or expansion stroke. If it opens too late, there is still excess pressure in the cylinder at the bottom dead centre (BC). This pressure resists the piston movement early in the exhaust stroke and increases the pumping work to push the exhaust gas from the cylinder. The closing time of the exhaust valve is also important. If the exhaust valve is closed too early, an excess of exhaust gases is trapped in the cylinder, and thus, the volumetric efficiency decreases. Also, the cylinder pressure would go up near the end of the exhaust stroke, causing a loss of net work from the engine. If the exhaust valve is closed late, there is an excess of overlap, with more backflow of exhaust gas into the intake [29].

Fig. 10a shows the pressure-time histories in the cylinder, in the exhaust manifold and in the intake manifold of the V12 engine. The mass flow rates through the valves of the engine are shown in Fig. 10b. The following can be drawn from these figures: a strong residual gas compression before TC back flows through the inlet valve at the beginning and at the end of the intake stroke. As mentioned already, the residual gas compression before TC causes a loss of net work from the engine. Especially, the back flow at the beginning of the intake stroke can be an explosion danger for this mixture loaded natural gas engine, since the exhaust gases are still hot.

The valve lift profiles as basic variant are shown in Fig. 10c. In order to obtain the effect of valve timing on the engine performance, a parametric study is accomplished. To do this, the valve

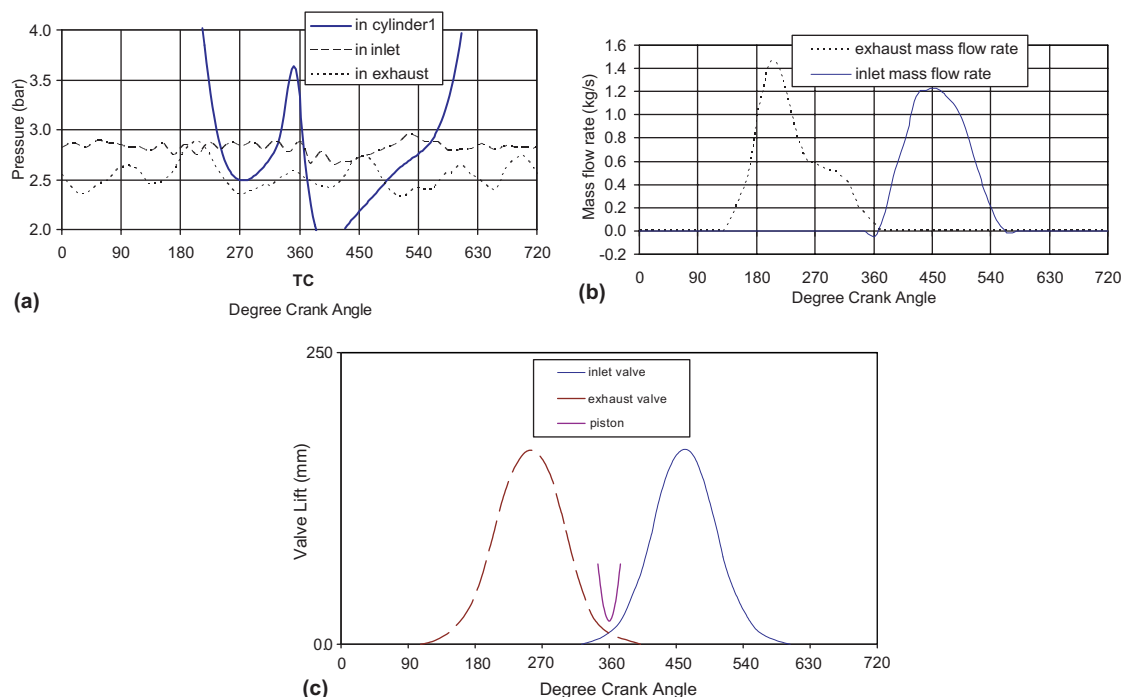


Fig. 10. (a) Pressure-time histories in exhaust, in cylinder and in inlet, (b) mass flow rates through valves for cylinder 1, (c) valve lift profiles.

lift profiles are left unchanged but shifted in both directions with an interval of  $10^\circ$  crank angle (dCA). This means that the cam profiles and cam lengths are left unchanged.

For this parametric study, the amount of fuel supplied to the engine and the exhaust turbine cross sectional area are left constant. These assumptions are necessary to obtain only the effect of valve timing. For optimization of the valve timing, the objective is to obtain the highest engine efficiency under the conditions of a trapping efficiency of 100% and no back flow through the valves.

For the discussion here, the following abbreviations are used:

EVO/EVC: Exhaust valve opening/closing.

IVO/IVC: Intake valve opening/closing.

The results are shown in Fig. 11 regarding volumetric efficiency, residual gas fraction, engine efficiency and trapping efficiency.

*Volumetric efficiency.* Fig. 11a shows that the volumetric efficiency rises always with the later opening of both intake and exhaust valves. If the intake valve opens later than 353 dCA, the

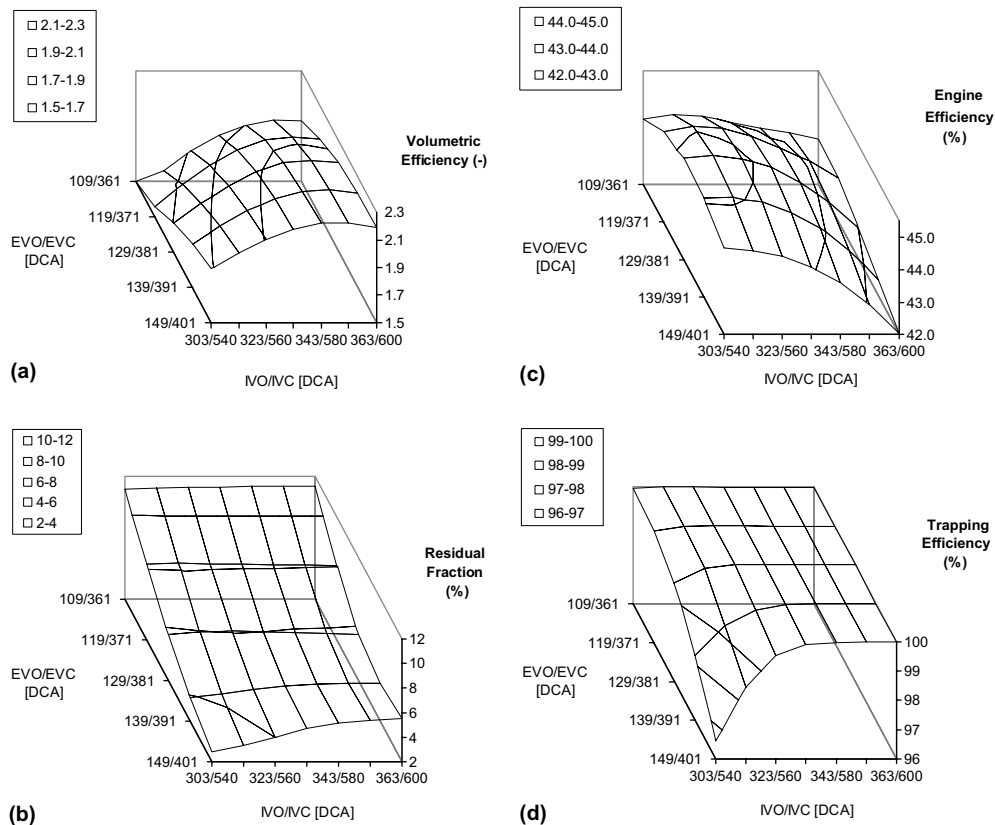


Fig. 11. Effect of valve timing on (a) volumetric efficiency, (b) residual fraction, (c) engine efficiency and (d) trapping efficiency.



volumetric efficiency drops again. The highest volumetric efficiency is obtained with the following valve timing combination: EVO = 149 dCA and IVO = 353 dCA. With this valve timing, a relatively small back flow into the inlet channel occurs.

**Residual fraction.** As shown in Fig. 11b, the residual fraction is strongly dependent on the EVO. With the earlier EVO, the residual fraction is getting higher. The influence of the inlet valve timing is only of subordinated importance as expected. The residual fraction changes in a wide range, and thus, an internal recycling of exhaust gases occurs without additional lines etc. This is an important result for future improvements of the engine regarding exhaust gas emissions.

**Engine efficiency.** Fig. 11c shows clearly that the engine efficiency has a maximum with the valve timing for EVO = 129 dCA and IVO = 313 dCA. With this valve timing, an increase of 0.84% point in engine efficiency is possible compared to the basic variant. If the efficiency is considered as the choice criterion, this valve timing would be optimum.

**Trapping efficiency.** As shown in Fig. 11d, with the earlier IVO and later EVO, the trapping efficiency is getting smaller than 100%, since the valve overlap period in this case becomes longer. As noted already, a trapping efficiency of 100% is the aim.

**Mass flows through valves.** To ensure there is no back flow through the valves, the mass flows through the valves for all valve timing combinations studied here are observed. This observation is a must to eliminate the valve timing combinations that give back flows. Fig. 12a shows that the

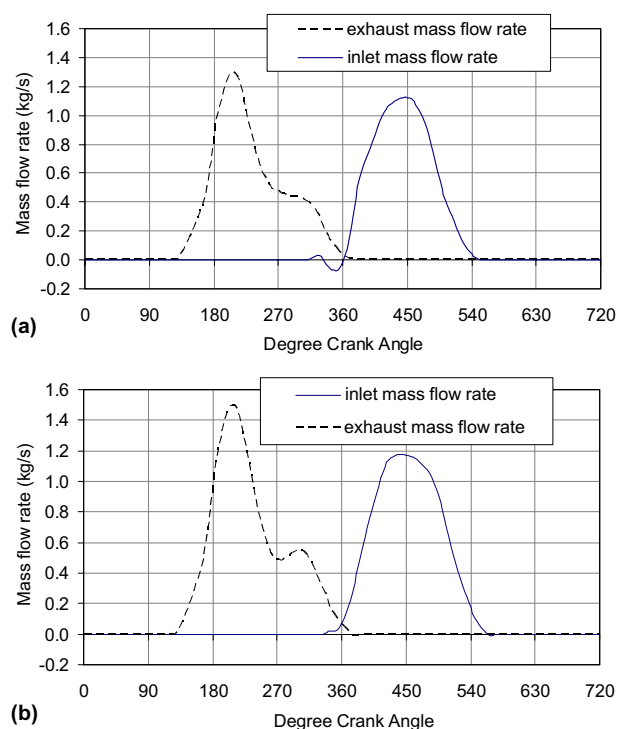


Fig. 12. (a) Mass flow rates for valve timing combination at which the highest engine efficiency is available. (b) Mass flow rates for the optimized valve timing.

valve timing at which the highest engine efficiency is reached gives a back flow at the beginning of the intake stroke. Thus, this valve timing is eliminated for optimization.

Since this observation showed that all valve timing combinations give a back flow into the intake channel, another investigation to optimize valve timing is made. As mentioned before, the investigations discussed already are accomplished while the valve lift profiles are left unchanged. For further optimization of the valve timing, additional valve timing combinations with different valve lift profiles and also with different cam profiles and cam lengths are investigated to find a favorable compromise regarding higher engine efficiency, a residual fraction of 100% and no back flow into the inlet channel. These objectives are achieved as a result of this additional investigation. The optimization of valve timing is accomplished with an exhaust manifold diameter of 132 mm. As mentioned in Section 9.2, the exhaust manifold diameter for the V12 engine is to be 0.9 times the cylinder bore. By enlargement of the exhaust manifold diameter from 132 mm to 170 mm, an additional increase of 0.21% point in engine efficiency is obtained. Fig. 12b shows the mass flows through the valves for the optimized valve timing. Note that there is no back flow with this valve timing. A comparison of the engine performance for three valve timing combinations, i.e. basic variant and optimum valve timing, is represented in Table 6. This comparison shows that the valve timing optimized here together with the optimized exhaust manifold diameter gives an increase of 0.85% point in engine efficiency.

### 10.2. Effect of valve lift profiles

The most significant flow restriction in an internal combustion engine is the flow through the intake and exhaust valves. Intake valves offer the greatest restriction to the incoming charge into the cylinder. To reduce this restriction, the intake valve diameter is to be increased. Also, the exhaust valves should be as large as possible, considering all other demands in the design of the combustion chamber. A larger valve gives a greater flow area and reduces the time of exhaust blow down. This allows for a later exhaust valve opening and a longer expansion stroke with less lost work [29].

There are three possibilities to decrease the flow restriction of the valve: Designing a larger valve lift which gives a greater area under the valve lift profile, increasing the valve diameter and increasing the valve flow coefficients via a well designed whole cylinder head and valve channel. To obtain the effect of valve lift profiles on engine performance, three valve lifts are used

Table 6  
Comparison for valve timing combinations

Variable	Basic variant	Optimized
EVO/EVC/IVO/IV	129/381/343/580	129/391/333/576
Engine efficiency (%)	44.36	45.21
Vol. efficiency (–)	2.15	2.17
Trapping efficiency (%)	99.97	99.96
Tmax (K)	1868	1860
Residual fraction (%)	4.99	5.88
Back flow	Yes	No

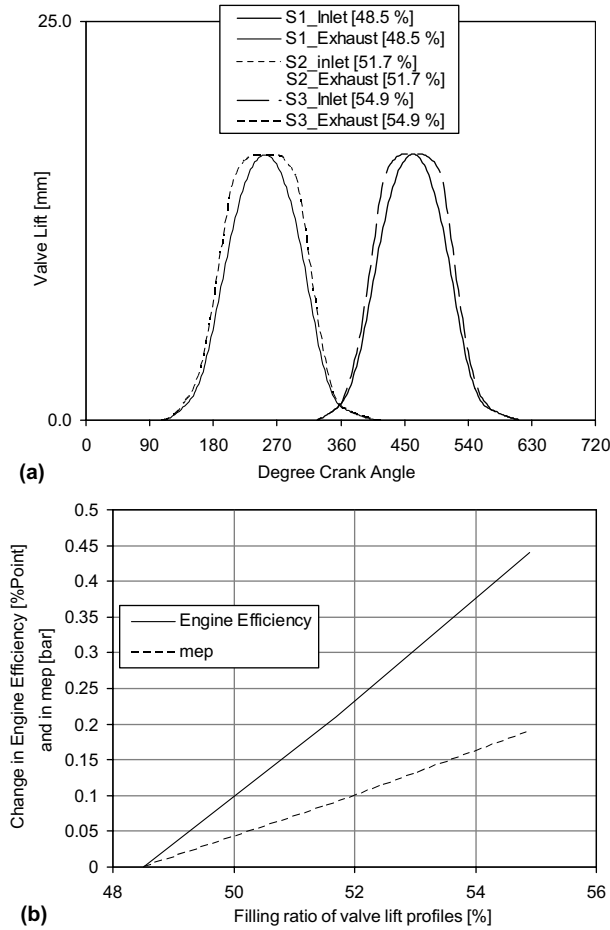


Fig. 13. (a) Valve lift profiles and (b) effect of valve lift profiles on engine performance.

(Fig. 13a). The basic variant S1 corresponds to the current valve profiles. On this basic variant, the variants S2 and S3 are generated. To obtain the influence of only valve profiles on the engine performance, the following are left unchanged: valve timing, maximum valve lift and valve lift profiles in valve overlap. Note that the fuel mass supplied to the cylinders is also left constant.

For this parametric study, a filling ratio for the valve lift profiles is defined as follows:

$$FG\_V = \frac{1}{\text{No. of Valves}} \sum_{i=1}^{\text{No. of Valves}} \left( \frac{F_{\text{VALVELIFT}}}{h_{V,\text{MAX}} \cdot \text{ODV}} \right)_i \quad (18)$$

where  $F_{\text{VALVELIFT}}$  is the area under the lift profile of the corresponding valve [mm dCA],  $h_{V,\text{MAX}}$  is the maximum stroke of the corresponding valve [mm] and ODV is the total opening time of the corresponding valve [dCA].

The filling ratios of the valve lift profiles S2 and S3 are 3.2% and 6.4% larger than that of S1, respectively. Fig. 13b shows clearly that the engine efficiency rises almost linearly with increasing

the filling ratio of the valves. The valve profiles S2 and S3 bring an increase of 0.21% and 0.44% in engine efficiency compared with S1, respectively.

It should be noted here that valves require a greater complexity of designing camshafts and mechanical linkages. Also, it is often necessary to have specially shaped cylinder heads and recessed piston faces just to avoid valve-to-valve or valve-to-piston contact [29].

### 10.3. Effect of exhaust valve diameter

To obtain the effect of exhaust valve diameter, a parametric study is investigated. For this investigation, the following are left unchanged: the exhaust valve lift profiles, exhaust valve flow

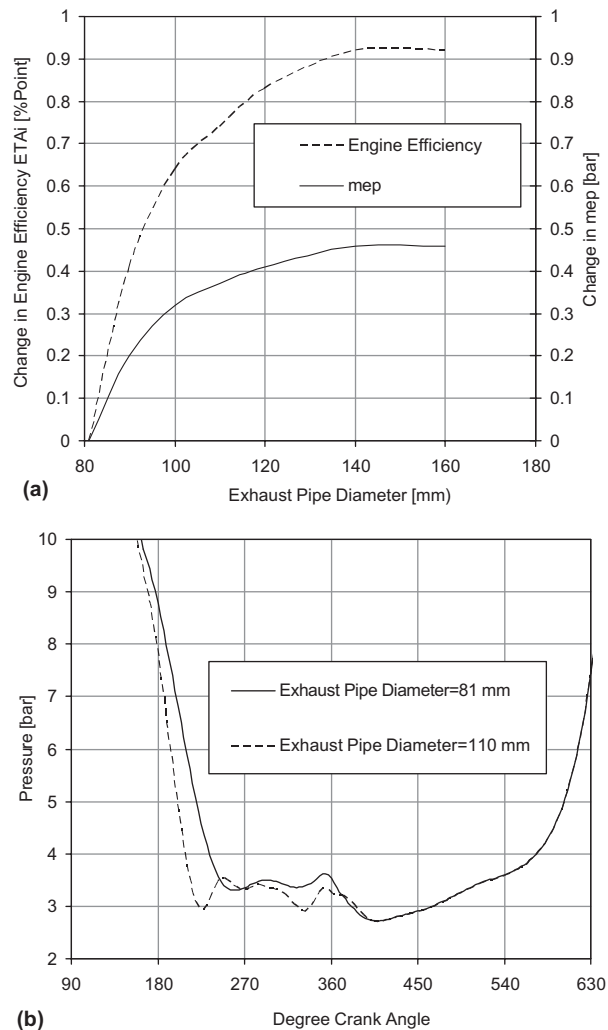


Fig. 14. Effect of exhaust valve diameter (a) on engine performance and (b) on cylinder pressure during gas exchange processes.

coefficients and exhaust valve timing. Only the exhaust valve diameter is varied. The corresponding channel diameter is also varied proportionally to the increasing of the exhaust valve diameter. The results in Fig. 14 show that the engine efficiency increases with increasing the exhaust pipe diameter. An increase of 10% in exhaust pipe diameter brings an increase of 0.4% in engine efficiency.

## 11. Conclusions

A study on the design of the exhaust system of a stationary natural gas engine is performed. Also the effect of the design on the engine performance is obtained. These investigations give very precise information for proper sizing of the inlet and exhaust pipe systems as well as the inlet and exhaust valves. The important issues of these investigations can be summarized as follows:

- In order to achieve an ideal constant pressure turbocharging, the diameter of the exhaust manifold is to be equal at least to the cylinder bore.
- Elongation of the exhaust pipes offers an improvement potential of the engine efficiency. Elongation of the pipes from 62 mm up to 1.5 m brings an efficiency increase of 0.38% points. However, elongation of the exhaust pipes has a few disadvantages like increasing the engine size and, thus, constructional complexity, which are a trade off between engine efficiency and compact engine size.
- A diffuser shaped T junction in the exhaust pipe system shows a clear improvement potential for the engine efficiency. The estimation for the increase of the engine efficiency from 1D as well as 3D simulations is around 0.3% points.
- For a higher engine efficiency, the valve timing must be optimized by considering volumetric efficiency, residual fraction, trapping efficiency and engine efficiency as well as by observing back flows into the inlet and exhaust channels. Also, the valve lift profiles are to be optimized.

## References

- [1] Chiavola O. Multi-dimensional CFD-transmission matrix modeling of IC engine intake and exhaust systems. *J Sound Vib* 2002;256(5):835–48.
- [2] Davies POAL, Harrison MF. Predictive acoustic modeling applied to the control of intake/exhaust noise of internal combustion engines. *J Sound Vib* 1997;202(2):249–74.
- [3] Lang O, Schorn N, Unger Th. Calculation investigations of design and optimisation of the charging system of large engines. In: Pischinger R, editor. Proceedings: 5. Tagung der Arbeitsprozess des Verbrennungsmotors, TU Graz; 1995. p. 211–38 [in German].
- [4] Nagumo S, Hara S. Study of fuel economy improvement through control of intake valve closing timing: cause of combustion deterioration and improvement. *JSAE Rev* 1995;16:13–9.
- [5] Kohany T, Sher E. Using the 2nd law of thermodynamics to optimize variable valve timing for maximizing torque in a throttled SI engine. SAE paper 1999-01-0328, 1999.
- [6] Gray C. A review of variable engine valve timing, SAE paper 880386, 1988.
- [7] Leone TG, Christenson EJ, Stein RA. Comparison of variable camshaft timing strategies at part load, SAE paper 960584, 1996.

- [8] Shiga S et al. Effect of early-closing of intake-valve on the engine performance in a spark-ignition engine, SAE paper 960586, 1996.
- [9] Moro D, Ponti F, Serra G. Thermodynamic analysis of variable valve timing influence on SI engine efficiency, SAE paper 2001-01-0667, 2001.
- [10] Sher E, Bar-Kohany T. Optimization of variable valve timing for maximizing performance of an unthrottled SI engine—a theoretical study. *Energy* 2002;27:757–75.
- [11] Goerg KA et al. Charge cycle calculation in the CAE concept. *MTZ* 1990;51(9):380–7 [in German].
- [12] Idelchik IE et al. Handbook of hydraulic resistance. Hemisphere Publishing; 1986.
- [13] Kuo TW, Khaligi B. Numerical study on flow distribution in T-junctions and a comparison with experiment, ICE-Vol. 23, Engine Modelling. ASME 1995. p. 31–8.
- [14] Klell M, Sams Th, Wimmer A. Calculation flows in T-junctions. *MTZ* 1998;59(12):844–51.
- [15] Meier E, Czerwinski J, Sreuli A. Thermodynamic comparison of various turbocharging systems with the help of characteristics. *MTZ* 1990:2 [in German].
- [16] Wehinger D et al. Handbook of engine process calculation program MOSES II. Inst F VKM U Thd, TU Graz, Austria, 1996 [in German].
- [17] BOOST, User Manuel for AVL BOOST, AVL List GmbH, Department for Applied Thermodynamics, 1996.
- [18] FIRE, Manual V6.2b, and V7.0, AVL-List GmbH, Austria, 1996.
- [19] Heywood JB. Internal combustion engine fundamentals. McGraw-Hill; 1988.
- [20] Kesgin U. Computational methods for optimization of gas exchange process of heavy duty gas engines. PhD Thesis, Technical University of Graz, Graz, Austria, 1996 [in German].
- [21] Kesgin U. Effect of the turbocharging system on the performance of a natural gas engine. *Energy Convers Manage* 2004;46:11–32.
- [22] Watson N, Janota MS. Turbocharging the internal combustion engine. The Macmillan Press; 1982.
- [23] Pischinger R, Krassnig G, Taucar G, Sams T. Thermodynamics of internal combustion engine. Berlin: Springer; 1989.
- [24] Ferguson CR. Internal combustion engines. John Wiley & Sons; 1986.
- [25] Launder BE, Spalding DB. Mathematical models of turbulence. Academic Press; 1972.
- [26] Menne R, Pischinger F. Improvements of effective efficiency of an exhaust channel for a turbocharged four-stroke diesel engine. *MTZ* 1984:1 [in German].
- [27] Gan G, Riffat SB. Numerical determination of energy losses at duct junctions. *Appl Energy* 2000;67:331–40.
- [28] Ferguson CR, Kirkpatrick AT. Internal combustion engines. 2nd ed. John Wiley & Sons; 2001.
- [29] Pulkrabek W. Engineering fundamentals of the internal combustion engine. Prentice Hall; 1997.